FACULTY OF PHYSICS, BABEŞ–BOLYAI UNIVERSITY
CLUJ-NAPOCA, ROMÂNIA

PHD THESIS SUMMARY

INTERFERENCE EFFECTS IN THE IONIZATION OF THE HYDROGEN MOLECULE

PÓRA MELINDA–KATALIN

SCIENTIFIC ADVISOR: PROF. DR. NAGY LADISLAU

JANUARY 2010

Contents of the Thesis

Keywords

- differential ionization cross section
- ionization of molecules
- hydrogen molecule
- semiclassical, impact parameter approximation
- interference effects

Introduction

Taking into consideration the wave character of the electron, and the two-center character of the hydrogen molecule with distance below 1Å between the two nuclei, we might consider that these two nuclei can be obstacles in the way of the wave associated to the ejected electron, in the ionization of the hydrogen molecule. This can be viewed as the two-slit Young experiment for the light. In the case of the hydrogen molecule the coherent emission source is represented by the two nuclei of the molecule, leading to interference-type oscillations in the ejected electron spectra.

In the last few years there were many experimental and theoretical studies about the ionization of the hydrogen molecule, and the observed interference effect in the ionization differential cross section. The ratio of the cross sections of the hydrogen molecule and two hydrogen atoms, as a function of the ejected electron velocity and ejection angle, presents an oscillating pattern. The transition amplitudes can be expressed as coherent superpositions of one-center amplitudes, displaying interference patterns in the cross section. These remain present even for cross sections averaged over the orientation of the axis of target molecule [1, 2]. Interference effects caused by the two-center character of a molecular target (H_2 or H_2^+) have been analyzed since a long time for charge transfer [1, 3, 4] and photoionization [2, 5].

In case of the ionization of the hydrogen molecule by fast charged particles there are several experimental results. In experiments, as projectile there were used high energy Kr^{34+} [6], Kr^{33+} [7], proton [8, 9], C^{6+} [10–13] and F^{9+} [14].

There are also theoretical results on this phenomena [15–26].

We developed a quite simple analytical theory for understanding and explaining the experimentally observed interference phenomena. Our theoretical analytical calculations [17] reproduced the interference effect, and gave a relatively good agreement with the experimental cross section. In order to improve the differential ionization cross section, to get a better agreement with the experimental results, we used another, numerical, method for the calculation of it.

Common in both theories is that the projectile has high energies, that is the reason why we assume for it a linear trajectory, while the particles from the target are treated with quantum mechanical formalisms. This is the semi-classical or impact-parameter approximation. The interaction between the projectile and the particle from the target is treated as a perturbation, because it influences the quantum state of the target.

In case of the photoionization the possibility of the interference effects in the ejected electron spectra due to the two-center character of a molecular target have been predicted for the first time by Cohen and Fano [5]. These phenomena have been analyzed in more detail by Walter and Briggs [2], including photodouble ionization.

Although there are many experimental data [27–30] and theoretical descriptions [31–36] for the photoionization of the hydrogen molecule, there are not many investigations on the interference effects. Cohen and Fano [5] and Walter and Briggs [2] were, who analyzed the interference effects in case of photoionization. There are only a few theoretical studies since then [19, 37–39].

The photoionization process may be treated in different gauges (using length, velocity or acceleration form of the dipole operator). If the wavefunction of the initial and the final states are exact (as it can be done easily for the H atom), results are gauge-independent. However, for atoms and molecules with more electrons, the electronic states cannot be described exactly, and usually the obtained results depend on the gauge. This is the case also for the relatively elaborate calculations done for the helium [40] or hydrogen molecule [33]. However, some approximations, as the random phase approximation (RPA) [33, 36] may lead to gauge-independent results.

2. Ionization of the hydrogen molecule by fast ion impact

2.1 Theoretical models for the ionization of the hydrogen molecule

We developed the models for hydrogen molecule target. Its particularity is that it is composed of two identical nuclei, which can be seen as two scattering centers by the emitted electron. The interaction of the projectile with the molecule is a time-dependent perturbation. In the semiclassical approximation the projectile motion is treated classically, the trajectory is a straight line.

Two models were developed for the ionization of the hydrogen molecule by fast ion impact. First the initial state is described as a linear combination of two $1s$ type atomic orbitals, and the final wavefunction is approximated with plane-waves. Using these wavefunctions we perform the calculations analytically. In the second approach the final continuum state is described by a more precise wavefunction, and the calculations are performed numerically.

2.1.1 Analytical calculations

The theoretical formulation follows closely the atomic target model of Hansen and Kocbach [42], here modified for molecular targets. The first order transition amplitude can be calculated knowing the initial and final wavefunction of the activ electron and the potential in what there are moving.

We assume the initial state of the electron in the hydrogen molecule to be a linear combination of two $1s$ type atomic orbitals centered at each of the nuclei, the final state wavefunctions for electrons of momentum $\mathbf{k}$ are approximated by plane waves. The evaluation of the amplitude is based on use of the Bethe integral for the potential, we performed the calculations using a peaking-approximation, i.e. only the fast emitted electrons are taken in consideration.

The transition probability for given impact parameter b and molecular axis orientation $\widehat{\mathbf{D}}$ in a simplified formula is

$$\begin{aligned} w(b,\widehat{\mathbf{D}}) &= |a(b,\widehat{\mathbf{D}})|^2 && (2.1)\\ &= c(b,\widehat{\mathbf{D}}) + g(b,\widehat{\mathbf{D}}) \cos\left[(k_{\|} - q) D \cos\theta_D\right], && (2.2) \end{aligned}$$

where $k_{\|}$ is the parallel component of the final momentum $\mathbf{k}$, relative to the projectile direction, q is the mininum momentum transfer.

For comparison with experiment the probabilities must be averaged over molecular orientation. The averaged probabilities can be integrated over the impact parameter to obtain the differential cross sections

$$\frac{d\sigma}{d\Omega_k dk} = 2\pi \int b\, w(b)\, db. \tag{2.3}$$

The integration (2.3) must be performed numerically. However, the interference pattern can be analyzed approximately, by recognizing that the most significant angular variation in (2.2) is contained in the fast oscillating factor of the interference term.

We average thus only this factor over the orientation of the molecular axis, assuming the other variations unimportant. This gives

$$\frac{1}{2}\int_0^{\pi} \cos\left[(q - k_{\|}) D \cos\theta_D\right] \sin\theta_D d\theta_D = \frac{\sin[(k_{\|} - q)D]}{(k_{\|} - q)D}. \tag{2.4}$$

Hence, the thus-approximated transition probability may be written in the form

$$w(b) = c(b) + g(b)\frac{\sin[(k_{\|} - q)D]}{(k_{\|} - q)D}, \tag{2.5}$$

and the corresponding cross section (2.3) is then

$$\frac{d\sigma}{d\Omega_k dk} = C + G\frac{\sin[(k_{\|} - q)D]}{(k_{\|} - q)D}. \tag{2.6}$$

This result can be contrasted to that obtained by Stolterfoht *et al.* [6],

$$\frac{d\sigma}{d\Omega_k dk} = C + G\frac{\sin kD}{kD}. \tag{2.7}$$

Since generally (for moderate values of ejected electron velocities) $q \ll k$, our approximate formula can be further approximated by

$$\frac{d\sigma}{d\Omega_k dk} = C + G\frac{\sin k_{\|}D}{k_{\|}D}. \tag{2.8}$$

2.1.2 Numerical calculations

The theory is based on the method presented in [41]. The initial state of H_2 is represented by a Heitler–London type molecular wavefunction with a fixed D distance between the two protons. The final state is the product of the bound-state wavefunction of the residual ion and the continuum-electron Coulomb-type wavefunction. Since the ionization process is fast relative to the nuclear motion, the final state of the residual ion is approximated by a H_2^+ wavefunction with the $\mathbf{D}$ vector of the initial H_2 state. The interaction between the activ electron and the projectile is a Coulomb-type interaction. Important steps in the calculation were that we applied the partial-wave expansion of the continuum-electron wavefunction, the Coulomb interaction was expanded into partial-wave series, and the target wavefunction which depends on the direction of vector $\mathbf{D}$ of the molecular axis was expanded into a Legendre series. Expressing the Legendre polynomials as a product of spherical harmonics the dependence on the direction $\widehat{D}$ of the molecular axis can be separated.

The transition probability is obtained by calculating the transition amplitude, knowing the initial and final wavefunctions of the active electron, using (2.1), and (2.3). Using the notations

$$\Gamma_{l_f l_c l_i}(k,R,D) = \int_{0}^{\infty} dr_1 r_1^2 R_{l_f}(kr_1) \frac{r_<^{l_c}}{r_>^{l_c+1}} c_{l_i}(r_1,D) \tag{2.9}$$

$$G^{m_c}_{l_f l_c l_i}(k,b,D) = \int_{-\infty}^{+\infty} dz\, e^{i\frac{\Delta E}{v}z} Y_{l_c m_c}(\widehat{R}) e^{-i m_c \varphi_b} \Gamma_{l_f l_c l_i}(k,R,D) \tag{2.10}$$

the differential cross section will be

$$\begin{aligned}
\frac{d\sigma}{d\Omega_k dk} &= \int_{0}^{\infty} |a(\mathbf{b},\mathbf{k},\mathbf{D})|^2 b\, db = 8\pi^3 \left(\frac{Z_p N_i}{v_p N_f}\right)^2 \\
&\times \sum_{l_f l_c l_i l_f' l_c'} \frac{i^{l_f'-l_f} e^{i(\sigma_{l_f'}-\sigma_{l_f})}}{(2l_i+1)\sqrt{(2l_f+1)(2l_f'+1)(2l_c+1)(2l_c'+1)}} \\
&\times (l_c 0 l_i 0|l_f 0)(l_c' 0 l_i 0|l_f' 0) \sum_{m_f m_c m_i} (l_c m_c l_i m_i|l_f m_f)(l_c' m_c l_i m_i|l_f' m_f) \\
&\times Y^*_{l_f m_f}(\widehat{k}) Y_{l_f' m_f}(\widehat{k}) \int_{0}^{\infty} G^{m_c}_{l_f l_c l_i}(k,b,D) G^{m_c\,*}_{l_f' l_c' l_i}(k,b,D)\, b\, db,
\end{aligned} \tag{2.11}$$

where $(lml'm'|LM)$ denotes a Clebsch-Gordan coefficient.

So we have the (2.6) and (2.11), two formulas for the differential ionization cross section. Using both formulas we calculate the cross section, investigate the interference effect, and compare our results with the experimental ones.

2.2 Results and discussions

We have studied the ionization of the H_2 and H_2^+ molecules. In the calculations the effective charge of the hydrogen molecule is α=1.165, the internuclear distance is D=1.42 (expressed in atomic units) and the ionization energy is 0.567 Hartree. In case of the H_2^+ the internuclear distance is D=2.00, the effective charge is α=1.00 and the ionization energy is 1.1 Hartree. We investigated the differential ionization cross section, using different projectiles and for different electron ejection angles and also investigated the interference effect. To enhance this effect the ratios of cross section for the hydrogen molecule over two hydrogen atoms are represented as a function of the ejected electron velocity for different ejection angles. The dependence of the differential cross section and the $\sigma(H_2)/2\sigma(H)$ cross section ratio over the molecular orientation was studied, too.

2.2.1 Analytical calculations

The theory and results of this model were published in *J. Phys. B: At. Mol. Phys.* [17]. The importance of this paper is that we predicted the angular dependence of the interference oscillations, which was proved later by experimental results.

Double differential ionization cross section

As a first step we made our calculation for the ionization of the hydrogen molecule by high energy Kr^{34+}, Kr^{33+}, H^+ projectiles. These projectiles were chosen because there are experimental results for these. In this summary I present our theoretical results along the adequate experimental results, for Kr^{34+} projectile, for the other projectiles the results are presented in the thesis.

The differential ionization cross sections of H_2 by 60 MeV/u Kr^{34+} impact for electron ejection angles 30° and 150°, as a function of the ejected electron energy, calculated from formula (2.2)–(2.3) are plotted along with the experimental data [6] in Fig. 2.1.

Because of the simplified final state and the peaking approximation valid only for high values of momentum k, for low electron energies these calculated cross sections are not expected to agree with the experiment. Some disagreement is found even at high electron energies. However, the model still is useful for understanding of the interference patterns.

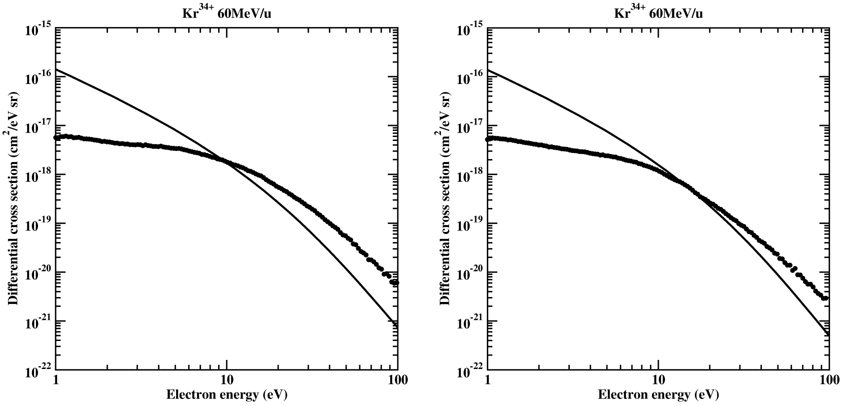

(a) $\theta_k = 30°$ (b) $\theta_k = 150°$

Figure 2.1: Double differential cross sections for the ionization of H_2 by 60 MeV/u Kr^{34+} ion impact for 30° (a) and 150° (b) ejection angles as a function of the electron energy. Present calculated values (solid line) are compared with the experimental data of Stolterfoht *et al.* [6] (full circles).

Interference effects

To emphasize the interference effect, following Stolterfoht *et al.* [6], we have calculated the cross section ratios for the hydrogen molecule and two hydrogen atoms. The cross sections for the atomic targets are evaluated with the same ionization potential and effective charge as for molecular targets.

To analyze the influence of the ejected electron scattering angle to the period and phase of the interference pattern the calculation were made for all ejection directions and up to 35 a.u. electron velocity. The results are plotted in Fig. 2.2. For these large velocities the ratio oscillates with a variable period, since the momentum transfer $q = (E_I + k^2/2)/v_p$ becomes comparable to k as the latter increases. As the simplified formula (2.6) predicts, the oscillations for smaller values of k at 90° ejection angle are suppressed, and the period of oscillations varies with the angle, as $2\pi/D\cos\theta_k$. The 'waves' on this three dimensional plot have an approximately constant 'wavelength' only in the z

direction.

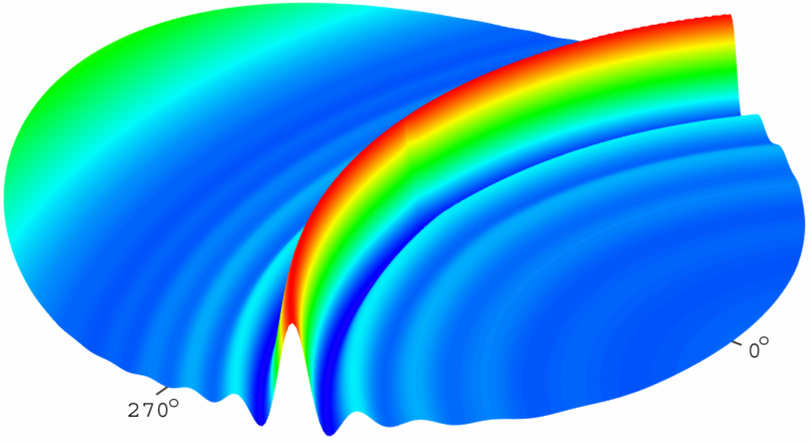

Figure 2.2: Calculated double differential cross sections ratios for the ionization of H_2 and 2H by 60 MeV/u Kr^{34+} ion impact as a function of ejection angle and electron velocity, where the velocity is used as radial coordinate. The maximum value of the electron velocity is 35 a.u.

The interference effect was studied experimentally [7] for the ionization of the hydrogen molecule by 68 MeV/u Kr^{33+} ion too. We made the calculations using the same energy and charge for the projectile, as in the experiment. The results are presented in Fig. 2.3 along the experimental values [7], for several ejection angles of the electron (see figure). The oscillations in cross section as a function of the ejected electron velocity have period and phase very close to the experimental values. This good agreement, as expected, is obtained for higher values of the ejected electron velocity ($v > 1.5$ a.u.).

The differential cross section ratios as a function of the ejected electron velocity and ejection angle relative to the projectile direction are plotted on Fig. 2.4. We can see a sharp maximum in the cross section ratio on the place of the binary peak. In case of 5 MeV energy projectile the binary peak in forward ejection is at $k \approx 28.24$ a.u., and decreases as the ejection angle groves to perpendicular direction. If we regard Fig. 2.2 we can't observe the

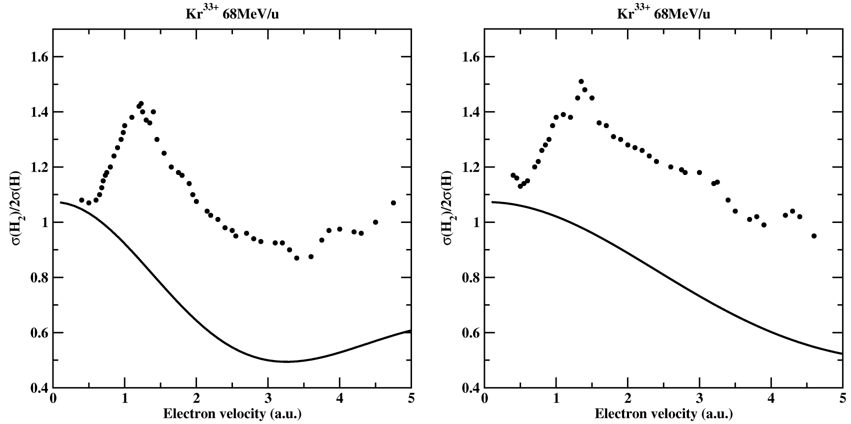

(a) $\theta_k = 30°$ (b) $\theta_k = 60°$

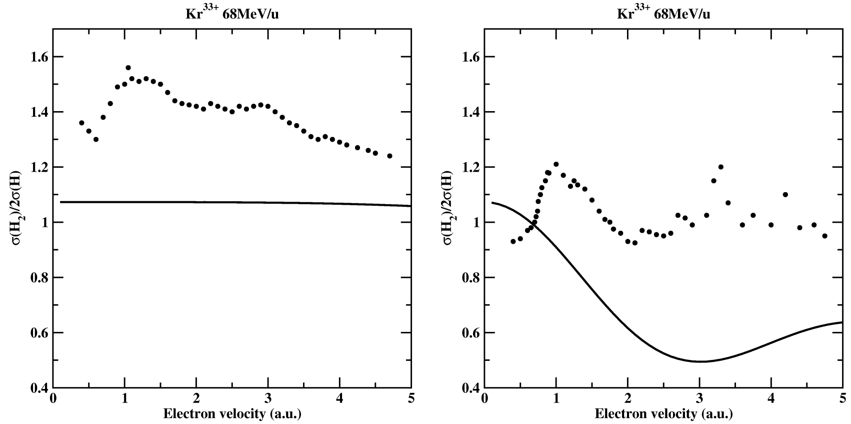

(c) $\theta_k = 90°$ (d) $\theta_k = 150°$

Figure 2.3: Double differential cross section ratios for 30° (a), 60° (b), 90° (c) and 150° (d) ejection angles (solid line) compared with the experimental ratios of Stolterfoht *et al.* [7] (full circles).

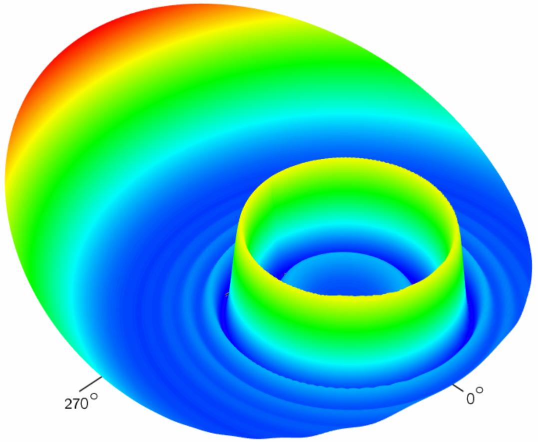

Figure 2.4: Theoretical results for $\sigma(H_2)/2\sigma(H)$ cross section ratios as a function of the ejected electron velocity and ejection angle, where the velocity is used as radial coordinate, in case of ionization of H_2 by 5 MeV H^+ projectiles. The maximum value of the electron velocity is 35 a.u.

binary peak for the forward direction range, because it should appear at $k \approx 98$ a.u., and we made our calculations up to 35 a.u. velocity.

Dependence on molecular orientation

In paper [16] Laurent *et al.* presents CDW-EIS (continuum distorted wave eikonal initial state) theoretical calculations, and studies the cross section dependence on the orientation of the molecule axis. Here the projectile is 13.7 MeV/u C^{6+}. These dependencies are investigated for 10 eV, 61.3 eV and 100 eV emitted electron energy. The axis of the molecule is parallel respectively perpendicular to the projectile direction. To compare our results with the published ones, we perform the calculations with our model using the same values for the energies and molecular orientations. To investigate the dependence over the molecular orientation in our calculation we skipped the integration over the axis directions. We calculate the cross section replacing (2.2) directly in (2.3), thus it will depend on the axis orientation. These results were published

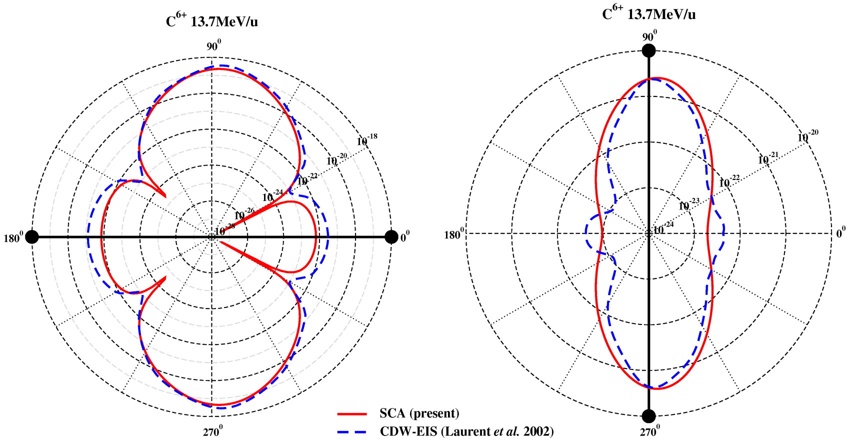

(a) $\theta_D = 0°$, $E_e = 100$ eV (b) $\theta_D = 90°$, $E_e = 100$ eV

Figure 2.5: Calculated double differential cross section for the ionization of H_2 by 13.7 MeV/u C^{6+} ion impact as a function of ejection angle along the CDW-EIS results [16]. The molecular axis is parallel (a) respective perpendicular (b) to the projectile trajectory. The ejected electron energy is 100 eV.

in *Nucl. Instrum. Meth. Phys. Res. B* [25].

In 2.5 polar graphs are plotted the CDW-EIS theoretical results of Laurent *et al.* [16] for parallel respective perpendicular axis orientation of the molecule with the projectile direction for 100 eV emitted electron energy, along our SCA theoretical results. As we can see in these graphs the orientation of the molecular axis influences the differential ionization cross section. Our results are in good agreement with the CDW-EIS theoretical calculation of Laurent *et al.* [16].

According to the above results we can declare that our simply model describes well the dependence over the molecular orientation.

Now let us focus on the influence of molecular axis orientation on the oscillation pattern observed in the cross section ratios as a function of ejected electron velocity. We made the calculations for higher electron velocities, up to 60 a.u., in order to get a better picture.

Fig. 2.6 presents the cross section ratio averaged over all φ_D angles, for

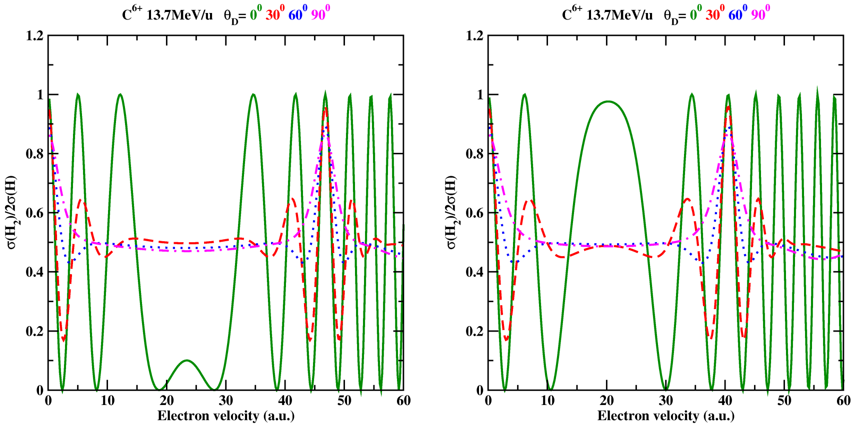

(a) $\theta_k = 0°$ (b) $\theta_k = 30°$

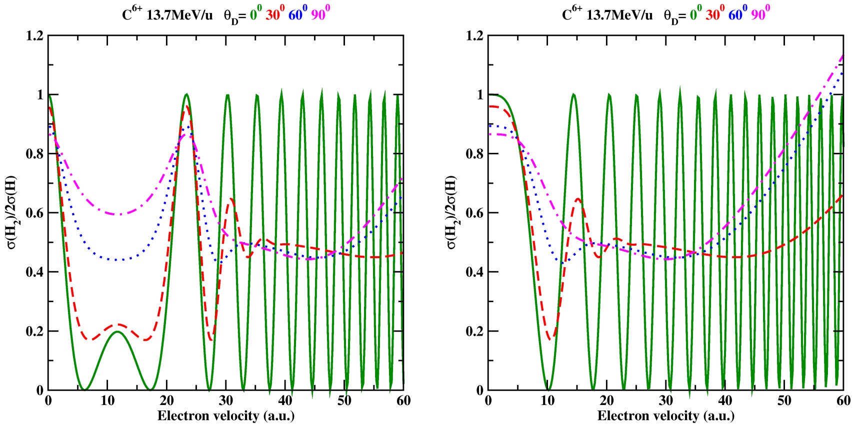

(c) $\theta_k = 60°$ (d) $\theta_k = 90°$

Figure 2.6: Ionization cross section ratio of the hydrogen molecule and two hydrogen atoms as a function of the ejected electron velocity for different θ_D angles and 0° (a), 30° (b), 60° (c) respective 90° (d) electron ejection angles.

different θ_D orientations of the molecular axis and different electron ejection angles. One may observe that the oscillations in the cross section ratio are the most pronounced for parallel orientation of the molecular axis relative to the beam direction in accordance with the findings of Sisourat *et al.* [43]. The interference is systematically found to be constructive (practically no θ_D dependence) when $k_{||} = q$, i.e. when the ejected electron velocity is $k \approx 2v \cos\theta_k$ ($k \approx 47$ a.u. for $\theta_k = 0°$, $k \approx 40$ a.u. for $\theta_k = 30°$ and $k \approx 23.5$ a.u. for $\theta_k = 60°$). In some cases, if the ionized molecule dissociates, the θ_D angle becomes experimentally detectable, and comparison of our predictions with the experiments may be possible.

In conclusion, we have investigated the influence of molecular orientation on the interference pattern. We have observed that at certain ejected electron velocities the interference is totally destructive. The orientation of the molecule has strong influence on the observed interference pattern in the differential ionization cross section of the hydrogen molecule.

2.2.2 Numerical calculations

If we take a look at the results with the analytical model we can see, that reproduces well the interference effect in the ionization of the hydrogen molecule, i.e. the phase and the period of the oscillations are in good agreement with the experimental results. The results of the differential cross sections differ from the experimental values. We tried an other model to calculate the differential cross section. Using the (2.11) differential cross section we made the calculations using the same projectiles as in previous model, in order to decide which model reproduces better the experiments.

In the partial-wave expansion of the continuum-electron wavefunction, the higher limit for the l_f was choosen depending on the value of the ejected electron energy. This limit is 6 for small electron energies and goes up to 30 for high energies.

We made the calculations using 60 MeV/u Kr^{34+} projectile and studied the differential ionization cross section, respective the cross section ratios of hydrogen molecule and two hydrogen atoms at 30° and 150° electron ejection angles, for 68 MeV/u Kr^{33+} projectile at 30° and 90° electron ejection angles. The results were published in *Technical Review (Physics)* [23].

Double differential ionization cross section

Fig. 2.7 presents the differential cross section of the hydrogen molecule in case of ionization by 60 MeV/u Kr^{34+} projectile together with the experimental results [6], for 30° (a) and 150° (b) electron ejection angles. We can see that this model gives a better agreement with the experimental results at low energies of the ejected electron for this projectile.

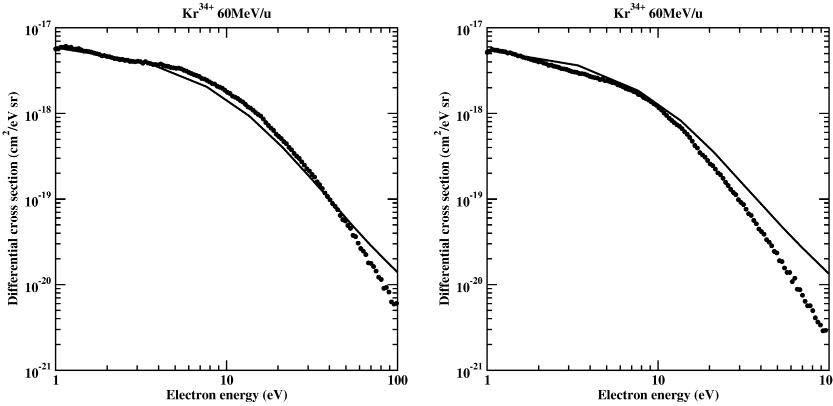

(a) $\theta_k = 30°$ (b) $\theta_k = 150°$

Figure 2.7: Differential cross section as a function of the ejected electron energy for ionization of H_2 by 60 MeV/u Kr^{34+} projectile at 30° (a) and 150° (b) electron ejection angles. Our theoretical results (solid line) are plotted along the experimental ones [6] (full circles).

From the Fig. 2.7 it can be seen, and others presented in the thesis, that this model describes the differential cross section at low energies of the electron better than our previous (analytical) one. At high energies there are discrepancies between our theoretical results and the experimental data. The cause of this difference is the one-center character of the final wavefunction. Next stepis to investigate the interference effect calculated from this second model.

Interference effects

To enhance the interference effect we plotted the $\sigma(H_2)/2\sigma(H)$ ratio as a function of the ejected electron velocity for different ejection angles and different projectiles.

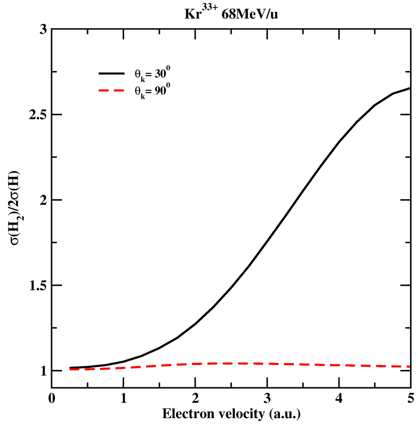

Figure 2.8: Theoretical results for the cross section ratio as a function of ejected electron velocity of H_2 for different electron ejection angles.

Fig. 2.8 presents the cross section ratios for 68 MeV/u Kr^{33+} projectile, for 30° and 90° ejection angles of the electron as a function of the ejected electron velocity. In this figure it can be seen, that there is an interference pattern, but the ratios have an increasing aspect. In order to avoid the increasing aspect of the cross section ratio with velocity and to compare the interference pattern with the experimental ones we fitted a straight line to our data, and with it we removed the overall increase of the ratio. In Fig. 2.9 we presented this new results along the experimental ones [7].

As it can be seen there is an oscillating pattern, but the period and the phase of the oscillation differs from the experimental values. This difference may be caused by the fact that the final one-centered wavefunction is not a good description of the final continuum-state.

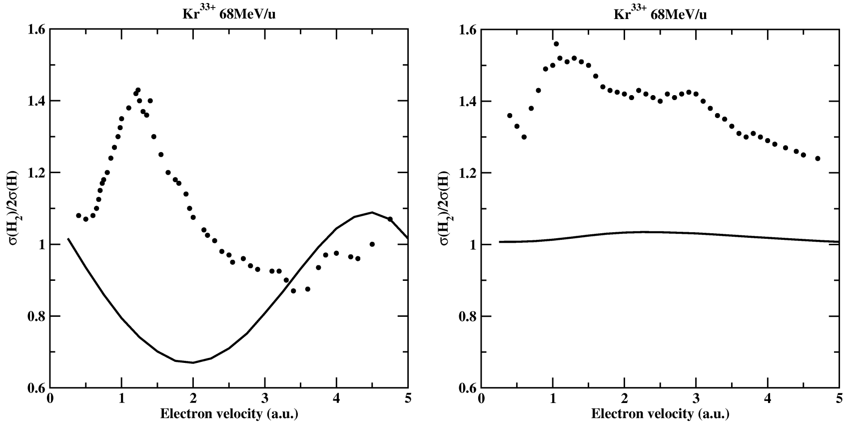

(a) $\theta_k = 30°$

(b) $\theta_k = 90°$

Figure 2.9: Corrected theoretical results for the cross section ratio as a function of ejected electron velocity of H_2 by 68 MeV/u Kr^{33+} projectile at 30° and 90° electron ejection angles (solid line) presented along the experimental data [7].

2.3 Conclusions

Whit the presented two models there were investigated not only the behavior of the differential cross section but also the interference effect due to the wave character of the electron. The interference effect is caused by the two center character of the hydrogen molecule. There were also investigated the effect of the orientation of the molecule in the space on the cross section and interference effects, respectively. We tried to find a suitable model which reproduce the experimental results.

These theories and results were published in several articles. The importance of the first, analytical model [17] was that we predicted the angular dependence of the period of oscillations, which was later proved by experimental results.

If we study the results obtained with our first model we can state, that it describes well the interference effect in case of the ionization of hydrogen

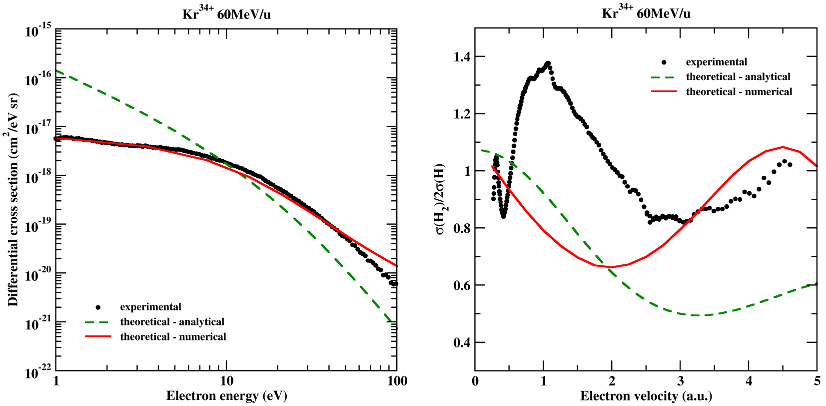

(a) cross section, $\theta_k = 30°$ (b) interference effect, $\theta_k = 30°$

Figure 2.10: Differential cross section as a function of the ejected electron energy (a) and cross section ratio as a function of ejected electron velocity (b) for ionization of H_2 by 60 MeV/u Kr^{34+} projectile at 30° electron ejection angles. Our theoretical (analytical respective numerical) results are plotted along the experimental ones [6].

molecule by different fast projectile ions. One may observe, that the period of the oscillations of the cross section ratio for the hydrogen molecule and two hydrogen atoms plotted as a function of the ejected electron velocity, changes with the scattering angle of the electron. Our results are in good agreement with the experimental ones. If we take a look at the differential cross sections, we can see that this model doesn't reproduce well the experimental results. There were made some studies on the dependence of the cross section and the interference pattern on the molecular axis orientation respective to the projectile trajectory. The studies were made for parallel and perpendicular orientation. The comparison of the results with the published ones reveals that the model is suitable even for the description of the dependence over the molecular axis orientation. The only weak point of the model is the magnitude of the differential cross section. To improve this disagreement we tried another model.

In order to compare the two models, in the second model we made our calculation for the same projectiles, with the same energy, and investigated the cross section and the interference effects for the same ejection velocities and angles of the electron.

As we can see in Fig. 2.10(a) we obtained a better agreement with the experimental results for the magnitude of the differential cross section at low electron energies with the numerical calculations. Regarding the interference effects, plotted in Fig. 2.10(b), we can say, that even with these results we can observe some oscillations in the cross section ratio, but the period and the phase does not fit the experimental ones. This differences may be explained by the fact that the one-centered wavefunction is not a good description for the final state.

In conclusion we can say, that we have theoretical models which can describe well the differential cross section, the interference effect and their dependence on the orientation of the molecular axis.

3. Photoionization of the hydrogen molecule

3.1 Photoionization in plane wave approximation

In order to express the interference patterns by simple analytic formula, we have described the ejected electron by plane waves. This may seem a too simplistic approach, and does not produce reliable values for the absolute cross section, but makes possible to emphasize the interference effects. We analyze the character of the results using both velocity and length forms of the dipole operator.

The differential photoionization cross section for a linearly polarized radiation may be expressed as

$$\sigma_{fi} = \frac{4\pi^2}{\omega_{fi} c} |M_{fi}(\omega_{fi})|^2, \tag{3.1}$$

and the matrix element in dipole approximation is

$$M_{fi}(\omega_{fi}) = \langle f | \boldsymbol{\epsilon} \nabla | i \rangle. \tag{3.2}$$

In order to calculate the matrix element M_{fi} we need the initial and final wavefunctions. In case of hydrogen atom final state f approximated by plane waves. For the hydrogen molecule we use a molecular orbital description. The initial state of the active electron in the hydrogen molecule is approximated by linear combination of two $1s$ type atomic orbitals and the final state wavefunction is a plane wave.

The use of plane waves makes possible to perform the calculations analytically. More accurate wavefunction require numerical calculations. The interference effects obtained by the use of plane waves will give only a qualitative description.

To verify if there is interference effect in the ionization cross section of the hydrogen molecule we have to calculate the ratio of the cross section of hydrogen molecule and two hydrogen atoms. To do this, first we have to obtain the cross section separately for the hydrogen atom and hydrogen molecule.

In order to obtain the ionization cross section we have to calculate the matrix element first.

3.1.1 Calculations in velocity form

In velocity form, the matrix element in dipole approximation is

$$M_{fi} = ik^{1/2}\boldsymbol{\epsilon}\langle f|\nabla_r|i\rangle, \tag{3.3}$$

where the $k^{1/2}$ factor is present because of the continuum wavefunction's normalization to the momentum.To verify if there is interference effect in the ionization cross section of the hydrogen molecule we have to calculate the ratio of the cross section of hydrogen molecule and two hydrogen atoms. To do this, first we have to obtain the cross section separately for the hydrogen atom and hydrogen molecule.

Hydrogen atom

Replacing the initial and final wavefunctions in the (3.3) matrix element, performing the calculations we obtain for the matrix element, and introducing in (3.1) and we get the ionization cross section in case of hydrogen atom

$$\sigma_{fi} = \frac{32}{\omega_{fi}c} \frac{\alpha^5 k^3}{(\alpha^2 + k^2)^4} \cos^2 \theta_\epsilon \tag{3.4}$$

with $\cos \theta_\epsilon = \boldsymbol{\epsilon} \widehat{\mathbf{k}}$.

Hydrogen molecule

For the hydrogen molecule we replace initial and final wavefunctions in the matrix element, averaging the thus obtained matrix element over all molecular orientation and and introducing in (3.1) the ionization cross section for photoionization of hydrogen molecule in velocity form will be

$$\sigma_{fi} = \frac{64}{\omega_{fi}c(1+S)} \frac{\alpha^5 k^3}{(\alpha^2 + k^2)^4} \cos^2 \theta_\epsilon \left[1 + \frac{\sin(kD)}{kD} \right]. \tag{3.5}$$

The $\sigma_{fi} \propto (\boldsymbol{\epsilon}\mathbf{k})^2[1+\frac{\sin(kD)}{kD}]$ for the photoionization of the hydrogen molecule in velocity form was first predicted by Cohen and Fano [5].

3.1.2 Calculations in length form

In dipole approximation the matrix element in length form is

$$M_{fi} = -k^{1/2} \omega_{fi} \boldsymbol{\epsilon} \langle f | \mathbf{r} | i \rangle. \tag{3.6}$$

The factor $k^{1/2}$ occurs if the continuum wavefunction is normalized to momentum.

We perform the same steps in the calculation of the ionization cross section as in case of the velocity form.

Hydrogen atom

$$\sigma_{fi} = \frac{512\omega_{fi}}{c} \frac{\alpha^5 k^3}{(\alpha^2 + k^2)^6} \cos^2 \theta_\epsilon \tag{3.7}$$

with $\cos\theta_\epsilon = \boldsymbol{\epsilon}\widehat{\mathbf{k}}$.

Hydrogen molecule

$$\begin{aligned}
\sigma_{fi} \quad = \quad & \frac{1024\omega_{fi}}{c(1+S)}\frac{\alpha^5 k^3}{(\alpha^2+k^2)^6}\cos^2\theta_\epsilon\left[1+\frac{\sin(kD)}{kD}\right]+ \\
& +\frac{16\omega_{fi}}{c(1+S)}\frac{\alpha^5 k}{(\alpha^2+k^2)^4}\left[\frac{D^3}{3}-D^2\cos^2\theta_\epsilon\frac{\sin(kD)}{kD}+\right. \\
& \left.+\frac{1}{k^2}\left(1-3\cos^2\theta_\epsilon\right)\left(\cos(kD)-\frac{\sin(kD)}{kD}\right)\right]+ \\
& +\frac{256\omega_{fi}}{c(1+S)}\frac{\alpha^5 k}{(\alpha^2+k^2)^5}\cos^2\theta_\epsilon\left[\frac{\sin(kD)}{kD}-\cos(kD)\right]. \qquad (3.8)
\end{aligned}$$

Now we have the formula for the ionization cross section in different gauges for the hydrogen atom, and for the hydrogen molecule. In the next chapter will be presented the results of the calculations, the discussion over these results.

3.2 Results and discussions

Hydrogen atom

First let have a look on the cross section of hydrogen atom in length form (3.7) and in velocity form (3.4). Taking into account that for a one-electron atom $\omega = \frac{k^2}{2}+\frac{\alpha^2}{2}$, one observes that in length form the cross section is exactly 4 times larger than in velocity form. The asymptotic behavior for high photon energies in both gauges is the correct $\sigma \propto \omega^{-7/2}$. Comparing these findings to the exact result obtained with Coulomb wavefunctions, which is gauge-independent [44] we may state, the plane-wave approximation leads to the correct result for high photon energies only in velocity gauge (see Fig. 3.1).

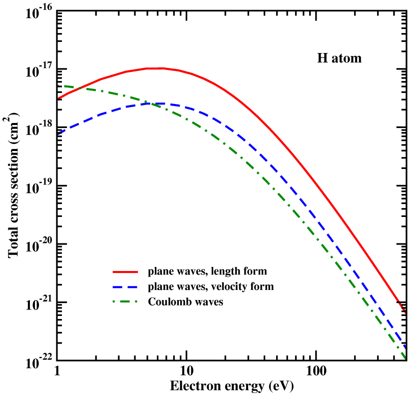

Figure 3.1: Total photoionization cross section for the hydrogen atom as a function of the ejected electron energy. The exact results (using Coulomb waves) are compared with the cross sections obtained by a plane wave approximation for the continuum electron in two different gauges.

Hydrogen molecule

If we study the cross sections for hydrogen molecule in length form (3.8) and in velocity form (3.5) we may observe that not only the magnitude of the cross section is different (observed also for atoms), but its dependence on the orientation of the molecular axis and on the ejection angle differs, too, in the two gauges. While in velocity form for molecules one obtains the same $\cos^2\theta_\epsilon$ angular dependence as for atoms, in length form we obtain a more complicated dependence, and there is electron ejection even for θ_ϵ=90°

The polar graphs on Figs. 3.2, 3.3 show differential cross sections for the photoionization of the hydrogen molecule for various photon energies and fixed orientation of the molecular axis, normalized to the maximum value. The cross section in length respective velocity form are represented along the random phase approximation (RPA) results of Semenov and Cherepkov [36], and the few available experimental data [44].

In Fig. 3.2 is represented the cross section for the molecular axis parallel to the polarization vector $\boldsymbol{\epsilon}$. At low photon energies all the results are in

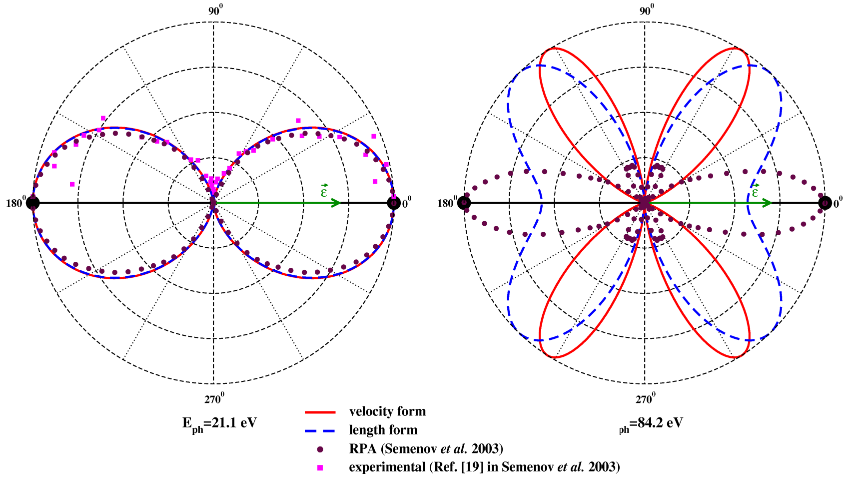

Figure 3.2: Polar representation of the differential photoionization cross section H_2 for the molecular axis parallel to the polarization vector, for different photon energies, along the RPA results of Semenov and Cherepkov [36] and few experimental data [45]. Cross sections are normalized to the maximum value.

good agreement with each other, length and velocity forms lead to the same angular distribution. This distribution is a typical dipole one, governed by $\cos^2\theta_\epsilon$. Discrepancy begins to occur at higher energies, the difference between the three models at 84.2 eV are already essential. At this energy the probability of ejecting an electron at 0 degrees relative to the polarization vector (and to the molecular axis) in velocity form becomes very small, because $\cos(kD/2)$ is close to 0 (being exactly 0 at 82 eV). The shape of the polar graph in length form is somehow different, because it does not reduces to zero at 0 degrees, but disagreement with the RPA results of Semenov and Cherepkov [36] is total – their differential cross section has a maximum value at 0 degrees.

If the molecular axis is perpendicular to the polarization vector, nothing interesting happens, our results for the angular distribution in the different gauges and those of Semenov and Cherepkov [36] are in perfect agreement (Fig. 3.3).

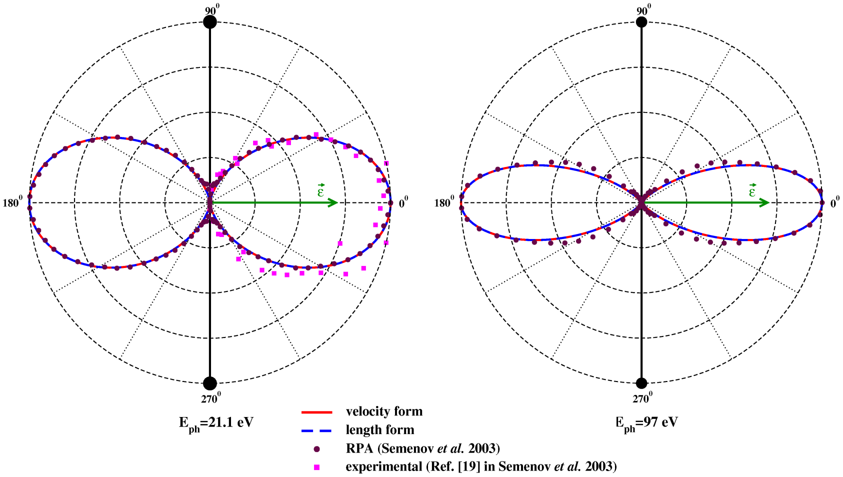

Figure 3.3: Same as Fig. 3.2, but for 90° between the molecular axis and the polarization vector.

The difference between the results obtained in the two different gauges may be also shown by the β asymmetry parameter, which characterizes the angular distribution

The asymmetry parameter in velocity form is constantly 2, as for the hydrogen atom, in length for is more complicated to calculate, and it is smaller then 2.

On Fig. 3.4 we have represented the asymmetry parameter in both gauges along with the RPA results of Cacelli *et al.* [33] and some experimental data [46, 47]. Our results in velocity form is constantly 2, but in length form the β value is lower and decreases with increasing photon energy. This behavior of the β parameter is similar to the RPA results of Cacelli *et al.* [33]. The obtained values in length form are closer to the experimental data and the RPA results, that our velocity form values.

Finally, in order to emphasize the interference effects in the photoionization due to the two-center character of the molecule, we have plotted on Fig. 3.5

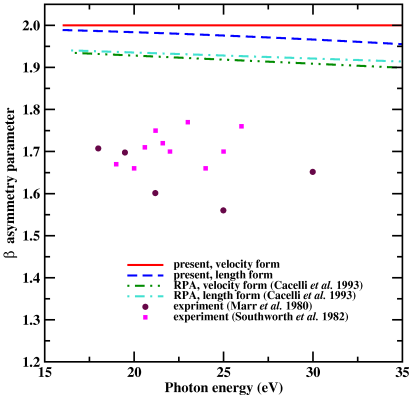

Figure 3.4: The β asymmetry parameter for the photoionization of H_2 as a function of the photon energy. The present calculation in velocity and length form are plotted along the RPA results in velocity and length form of Cacelli *et al.* [33], and experimental data of Marr *et al.* [47], and Southworth *et al.* [46]

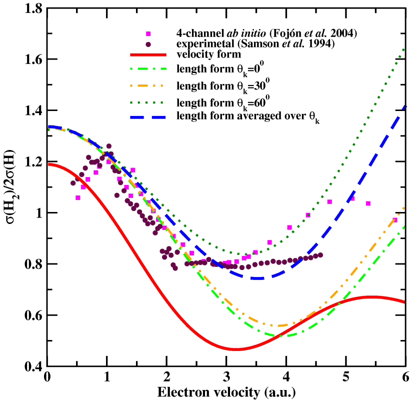

Figure 3.5: Photoionization cross section ratios $\sigma(H_2)/2\sigma(H)$ as a function of the ejected electron velocity. In length form the ratios are represented for different θ_k electron ejection angle relative to the projectile direction, and also for total ionization cross sections (or averaged over the angles).

the $\sigma(\mathrm{H}_2)/2\sigma(\mathrm{H})$ cross section ratio. This method, used first by Stolterfoht *et al.* [6] for the ionization by ion impact gives the possibility to observe oscillations in the molecular cross section, i.e., maxima and minima due to the interference. Our theoretical ratios are represented along the experimental photoionization cross section of the hydrogen molecule of Samson and Haddad [30] divided by the double of the theoretical total cross section of the hydrogen atom, using the same ionization potential for the atoms as for the molecule. Theoretical ratios are calculated using plane waves for the ejected electron in velocity and length forms. In this case the θ_k electron emission angle is related to the projectile direction, so the relation between θ_k and θ_ϵ is $\theta_k = \frac{\pi}{2} - \theta_\epsilon$. As may be observed from (3.5), in velocity form the differential cross section has the same angular distribution as for atoms, and the ratio does not depend on the electron ejection angle. This is not case for the length form (3.8), and the cross section ratio depends on the electron ejection angle. This ratio increases for higher velocities and angles close to 90°, where the cross section for atoms tends to 0.

In their RPA calculation, Semenov and Cherepkov [36] have found the $p\sigma$ component of the cross section a minimum around 80 eV photon energy, which they call 'Cooper-like'. They state, that this minimum is related to the non-spherical shape of the molecular potential. This is certainly true, but we can add, that this minimum is caused by the interference of the electron waves emitted by the two centers of the molecule. Recent studies [39] also showed that for homonuclear molecules the Cooper-minima and the Young-type interference minima appear at the same electron momentum.

In length form the differential cross section does not reach zero, but the minimum still exists. If one integrates over all possible orientations of the molecular axis, instead of the pronounced minimum observed for electrons ejected parallel to the molecular axis, one observes a broad minimum shifted to higher energies (see Fig. 3.5). The minimum is obtained at higher electron velocities in length form than in velocity form. The cross section ratios obtained in length form fits very well the experimental ratios.

3.3 Conclusions

Interference effects caused by the two-center character of the target in the photoionization of the hydrogen molecule have been studied. These results were published in *Phys. Lett. A* [38]. In order to express the factors in the cross section due to the interference in closed analytic form, we have approximated the final state of the ejected electron by plane waves. In these conditions the calculations performed in different gauges lead to different results for the absolute value of the cross section and angular distributions of the ejected electron. For the absolute value, velocity form lead to better results (cross sections obtained in length form are too high), but for the angular distribution length form seems to give more interesting and reliable results. When averaged over the orientation of the molecular axis, velocity form calculations give the same $\cos^2\theta_\epsilon$ angular distribution as for atoms [2], while in length form calculations lead to more complicated angular distributions. In the latter case there is possible the ejection of the electron even perpendicular to the polarization vector, as in case of the use of more evaluated wavefunctions [2].

As previously for ion impact [17], we have studied the ratio of the differential ionization cross sections for the hydrogen molecule and two hydrogen atoms as a function of ejected electron velocity. Maxima and minima are obtained as a clear evidence for the interference effects. These oscillations in velocity form do not depend on the ejection angle, as have been observed for ion impact. However in length form an angular dependence of the ratio have been observed, because of the different angular distribution of the photoelectron for the atom and the molecule. When integrated over the angles, our predictions obtained in length form for these oscillations are in good agreement with the experiments [30, 37].

4. Final conclusions

The thesis concentrates on the interference effect observed in the ionization differential cross section ratios of hydrogen molecule and two hydrogen atoms as a function of the ejected electron velocity, and for different electron ejection angles, for ionization by fast charged particle and photoionization. The interference effect is caused by the two-center character of the hydrogen molecule.

The calculations are based on the semiclassical impact parameter approximation. In this approximation the trajectory of the projectile is considered linear, and treated as a classical motion, the electrons of the target system is treated with quantum mechanical formalisms. The interaction between the projectile and the target's electrons is considered as a perturbation. We have calculated the differential ionization cross section of the hydrogen molecule in case of ionization by fast charged particles respective photoionization.

In case of ionization of the hydrogen molecule by fast ions we developed two models. In the first model the final wavefunction of the continuum electron is approximated by plane waves, so the calculations can be made analytically. In the second model the final wavefunction is calculated numerically, and is a Coulomb-type wavefunction.

We made the calculations for the ionization of the hydrogen molecule, respective the hydrogen atom, with fast ions using both models and compared the obtained results with the experimental ones.

Analyzing the results obtained for the differential ionization cross section of the hydrogen molecule we can state that the second model, i.e. the numerical calculations, gives more precise results, the obtained data has better agreement with the experimental values as the ones obtained with the analytical calculations, especially for low energies of the ejected electron.

If we study the interference effect, we can notice that the analytical calculations gives better agreement with the experimental results. The oscillations in the interference pattern is the most pronounced in case of parallel orientation of the molecule respective to the projectile direction. The interference is systematically found to be constructive (practically no θ_D dependence) when $k_{\|} = q$, i.e. when the ejected electron velocity is $k \approx 2v \cos\theta_k$. The obtained results are in good agreement with the other published theoretical results.

Beside the ionization of the hydrogen molecule with fast charged particles we also studied the appearance of the interference effect in case of photoionization [38]. In this case we also described the active electron final state with plane waves.

We performed the calculations in different gauges, i.e. length and velocity gauge. The calculations performed in different gauges lead to different results for the absolute value of the cross section and angular distributions of the ejected electron. For the absolute value, velocity form lead to better results, but for the angular distribution length form seems to give more interesting and reliable results. When averaged over the orientation of the molecular axis, velocity form calculations give the same angular distribution as for atoms, while in length form calculations lead to more complicated angular distributions. In the latter case there is possible the ejection of the electron even perpendicular to the polarization vector, as in case of the use of more evaluated wavefunctions.

Analyzing the interference pattern we observed that in velocity form, the oscillations are independent of the electron ejection angle, while in length form the dependence on the ejection angle is present. Averaging over the electron ejection angles the oscillations also remains, and are in good agreement with the experiments.

In the present work the ionization of the hydrogen molecule by fast particle impact and photoionization was studied using different theoretical models. Our main objective was the investigation of the interference effect appearing in the double differential ionization cross section due to the two-center character of the hydrogen molecule. In both cases, charged particle and photon impact ionization, this effect was evinced. The obtained results are in good agreement with the experimental data and other theoretical findings.

Bibliography

[1] Corchs S.E. and Rivarola R.D., *Phys. Scr.* **50** (1994) 469

[2] Walter M. and Briggs J., *J. Phys. B: At. Mol. Phys.* **32** (1999) 2487

[3] T.F. Tuan, *Phys. Rev.* **117** (1960) 756

[4] S.E. Corchs, H.F. Busnengo and R.D. Rivarola, *Nucl. Instrum. Meth. Phys. Res. B* **149** (1999) 247

[5] H.D. Cohen and U. Fano, *Phys. Rev.* **150** (1966) 30

[6] N. Stolterfoht, B. Sulik, V. Hoffmann, B. Skogvall, J.Y. Chesnel, J.Rangama, F. Frémont, D. Hennecart, A. Cassimi, X. Husson, A.L. Landers, J.A. Tanis, M.E. Galassi and R.D. Rivarola, *Phys. Rev. Lett.* **87** (2001) 023201

[7] N. Stolterfoht, B. Sulik, L. Gulyás, B. Skogvall, J.Y. Chesnel, F. Frémont, D. Hennecart, A. Cassimi, L. Adoui, S. Hossain, J.A. Tanis, *Phys. Rev. A* **67** (2003) 030702

[8] S. Hossain, A.S. Alnaser, A.L. Landers, D.J. Pole, H. Knutson, A. Robinson, B. Stamper, N. Stolterfoht, and J.A. Tanis, *Nucl. Instrum. Meth. Phys. Res. B* **205** (2003) 484

[9] S. Hossain, A. L. Landers, N. Stolterfoht, and J. A. Tanis, *Phys. Rev. A* **72** (2005) 010701

[10] Deepankar Misra, U. Kadhane, Y.P. Singh, L.C. Tribedi, P.D. Fainstein and P. Richard, *Phys. Rev. Lett.* **92** (2004) 153201

[11] Deepankar Misra, A. Kelkar, U. Kadhane, Ajay Kumar, Lokesh C. Tribedi, and P. D. Fainstein, *Phys. Rev. A* **74** (2006) 060701

[12] Misra D. et al, *Rad. Phys. Chem.* **75** (2006) 1723–1726

[13] Deepankar Misra, A. Kelkar, U. Kadhane, Ajay Kumar, Y. P. Singh, and Lokesh C. Tribedi, P. D. Fainstein, *Phys. Rev. A* **75** (2007) 052712

[14] Deepankar Misra, Aditya H. Kelkar, Shyamal Chatterjee and Lokesh C. Tribedi, *Phys. Rev. A* **80** (2009) 062701

[15] M.E. Gallasi, R.D. Rivarola, P.D. Fainstein, N. Stolterfoht, *Phys. Rev. A* **66** (2002) 052705

[16] G. Laurent, P.D. Fainstein, M.E. Galassi, R.D. Rivarola, L. Adoui and A. Cassimi, *J. Phys. B: At. Mol. Phys.* **35** (2002) L495

[17] L. Nagy, L. Kocbach, **K. Póra** and J.P. Hansen, *J. Phys. B: At. Mol. Phys.* **35** (2002) L453–L459

[18] **K. Póra**, L. Nagy, *Nucl. Instrum. Meth. Phys. Res. B* **233** (2005) 293–297

[19] L. Nagy, S. Borbély and **K. Póra**, *Braz. J. Phys.* **36** (2006) 511–514

[20] L. Sarkadi, *J. Phys. B: At. Mol. Phys.* **36** (2003) 2153–2163

[21] C.R. Stia, O. A. Fojón, P.F. Weck, J. Hanssen and R.D. Rivarola, *J. Phys. B: At. Mol. Phys.* **36** (2003) L257

[22] Tanis J.A. and Hossain S., *Nucl. Instrum. Meth. Phys. Res. B* **261**(2007) 226–229

[23] **Póra Katalin**, Nagy László, *Műszaki Szemle, Fizika szám* **41** (2008) 18–23

[24] S. Borbély, **K. Póra** and L. Nagy, *J. Phys: Conf. Series* **163** (2009) 012067

[25] **K. Póra**, L. Nagy, *Nucl. Instrum. Meth. Phys. Res. B* **267** (2009) 370–372

[26] F. Járai-Szabó, **K. Nagy-Póra**, L. Nagy, *J. Phys. B: At. Mol. Phys.* **42** (2009) 245203

[27] C. Backx, G.R. Wight and M.J. Van der Wiel, *J. Phys. B: At. Mol. Phys.* **9** (1976) 315

[28] J.A.R. Samson, *Phys. Rep.* **28** (1976) 303

[29] L.C. Lee, R.W. Carlson and D.L. Judge, *J. Quant. Spectrosc. Radiat. Transfer* **16** (1976) 873

[30] J.A.R. Samson and G.N. Haddad, *J. Opt. Soc. Am. B* **11** (1994) 277

[31] M.R. Flannery and U. Öpik, *Proc. Phys. Soc. (London)* **86** (1965) 491

[32] S.P. Khare, *Phys. Rev.* **173** (1968) 43

[33] I. Cacelli, R. Moccia and A. Rizzo, *J. Chem. Phys.* **98** (1993) 8742

[34] M. Yan, H.R. Sadeghpour and A. Dalgrano, *Astophys. J.* **496** (1998) 1044

[35] F. Martín, *J. Phys. B: At. Mol. Phys.* **32** (1999) R197

[36] S.K. Semenov and N.A. Cherepkov, *J. Phys. B: At. Mol. Phys.* **36** (2003) 1409

[37] O.A. Fojón, J. Fernandez, A. Palacios, R. D. Rivarola and F. Martin, *J. Phys. B: At. Mol. Phys.* **37** (2004) 3035

[38] L. Nagy, S. Borbély, **K. Póra**, *Phys. Lett. A* **327** (2004) 481

[39] R. Della Picca, P.D. Fainstein, M.L. Martiarena, N. Sisourat and A. Dubois, *Phys. Rev. A* **79** (2009) 032702

[40] S.P. Lucey, J. Rasch, C.T. Whelan, H.R.J. Walters, *J. Phys. B: At. Mol. Phys.* **31** (1998) 1237

[41] L. Nagy and L. Végh, *Phys. Rev. A* **46** (1992) 284–289

[42] J.P. Hansen and L. Kocbach, *J. Phys. B: At. Mol. Phys.* **22** (1989) L71–L77

[43] Nicolas Sisourat, Jérémie Caillat, Alain Dubois and Pablo D. Fainstein, *Phys. Rev. A* **76** (2007) 012718

[44] H. Hall, *Rev. Mod. Phys.* **8** (1936) 358

[45] Y. Hirosika, J.H.D. Eland, *private communication*, cited in [36]

[46] S. Southworth, W.D. Brewer, C.M. Truesdale, P.H. Kobrin, D.W. Lindle, D.A. Shirley, *J. Electron Spectrosc. Rel. Phenomena* **26** (1982) 43

[47] G.V. Marr, R.H. holmes, K. Kodling, *J. Phys. B: At. Mol. Phys.* **13** (1980) 283